The Journal of Neuroscience, November 1995, 15(11): 7238–7249

Early Patterns of Migration, Morphogenesis, and Intermediate Filament Expression of Subventricular Zone Cells in the Postnatal Rat Forebrain

Marielba Zerlin,[1] Steven W. Levison,[2] and James E. Goldman[1]

[1]Department of Pathology and the Center for Neurobiology and Behavior, Columbia University College of P&S, New York, New York 10032 and [2]Department of Neuroscience and Anatomy, Penn State College of Medicine, Hershey, Pennsylvania 17033

Recent studies using retroviral labeling of subventricular zone (SVZ) progenitors *in vivo* in neonatal rats have directly demonstrated the generation of both astrocytes and oligodendrocytes from these progenitors. In the present study, we used a recombinant retroviral vector encoding β-galactosidase, and analyzed brains within the first week after retroviral injection to trace the early routes that SVZ cells take as they migrate into white matter and cortex and characterized the early morphological and antigenic changes that accompanied their differentiation. SVZ cells follow specifically definable migratory routes as they colonize the cortex and subcortical white matter. Glial progenitors do not populate the cortex in a systematic, laminar fashion, as do neuroblasts. The abundance of labeled progenitors in radial arrangements and the close apposition of many immature cells to vimentin+ radial glial processes, suggest that glial progenitors migrate along radial glia. Labeled SVZ cells, which displayed a simple, unipolar or bipolar morphology, lacked detectable vimentin and nestin intermediate filaments. Similarly, β-galactosidase–positive cells in white matter lacked these filaments. In contrast, labeled, multipolar cells in the cortex, and a few of the immature-appearing cortical cells expressed nestin and vimentin. At these early time points, GFAP was not detected in β-galactosidase–labeled cells. Multipolar cells in cortex frequently displayed processes extending toward and contacting blood vessels. These observations suggest that the expression of nestin and vimentin occurs after progenitors emigrate from the SVZ and that filament expression and contact with blood vessels represent an early stage of astrocyte differentiation.

[Key words: subventricular zone, astrocytes, oligodendrocytes, glia, migration, nestin]

The progenitors for neurons and glia that comprise the CNS are located in two germinal zones: the ventricular zone (VZ), lining the cerebral ventricles, and the adjacent subventricular zone (SVZ). Neurogenesis takes place during embryonic life with a systematic laminar colonization of the developing cerebral cortex by postmitotic neuroblasts (Angevine and Sidman, 1961; Berry and Rogers, 1965; Hicks and D'Amato, 1968). Radial glial processes serve as guides for the migrating, immature neurons (Rakic, 1972; Hatten, 1990). In contrast to neurogenesis, the pattern of colonization of the cerebral hemispheres by glial progenitors is not well understood. Gliogenesis takes place largely during early postnatal life and coincides with a dramatic expansion of the SVZ. ^{3}H-Thymidine incorporation studies after short survival times have identified the SVZ as a highly proliferative zone during perinatal life (Altman, 1966; Paterson et al., 1973; Imamoto et al., 1978). After long survival times, the appearance of label in mature glia has supported the idea that the SVZ contains glial precursors. However, the mitotic dilution of label and the incorporation of label by glia residing outside of the SVZ makes the interpretation of results difficult. These complications, together with the fact that the SVZ is a large area makes the tracing of migratory routes by this approach complicated.

Studies with antibodies against glial antigens at different developmental stages were used to infer the origin of white matter oligodendrocytes to progenitors in the SVZ (Curtis et al., 1988; LeVine and Goldman, 1988a,b; Reynolds and Wilkin, 1988; Hardy and Reynolds, 1991). An SVZ origin of astrocytes could not be concluded, since no cells coexpressed both immature glial markers and the astrocyte marker, GFAP. Morphological studies using such various techniques and reagents as astroglia specific antibodies, Golgi impregnations, thymidine uptake, and DiI labeling have indicated the conversion of radial glia into astrocytes in late gestation and during postnatal life (Schmechel and Rakic, 1979; Misson et al., 1988; Voigt, 1989; Edwards et al., 1990) and have implied the generation of astrocytes from SVZ cells (Gressens et al., 1992).

Recent studies using retroviral labeling of SVZ progenitors *in vivo* in neonatal rats have directly demonstrated the generation of both astrocytes and oligodendrocytes from SVZ cells (Levison and Goldman, 1993; Levison et al., 1993; Luskin and McDermott, 1994). In previous work conducted in our laboratory, animals were analyzed after 4 weeks. By that time, the labeled progenitors had reached their final destinations and most of them had matured. In the present study, we utilized the same *in vivo* retroviral labeling technique, but analyzed brains within the first week after retroviral injection. This was done to attempt to trace the early routes that SVZ cells take as they migrate into

Received Apr. 19, 1995; revised June 26, 1995; accepted June 28, 1995.

We thank JoAnn Gensert for helpful advice with the immunofluorescence, Dr. Carol Mason for critical reading of the manuscript, and Dr. Martin Julius for valuable suggestions and discussions. This work was supported by NIH Grant NS17125.

Correspondence should be addressed to Dr. Marielba Zerlin, Department of Pathology, Columbia University College of P&S, 630 West 168th Street, New York, NY 10032.

white matter and cortex and to characterize early morphological and antigenic changes during glial differentiation. We find that labeled SVZ cells follow routes that are specifically definable in antero-posterior and medio-lateral directions. Furthermore, glial progenitors do not populate the cortex in a systematic, laminar fashion, as do postmitotic neuroblasts. However, the major routes of migration appear to be shared with neurons, and, like neurons, immature glia also use radial glial processes to ascend into the cortex. Additionally, our observations suggest that the expression of the intermediate filament proteins, nestin and vimentin, occurs after progenitors emigrate from the SVZ and represents an early stage of astrocyte differentiation.

Materials and Methods

Retrovirus stocks, stereotactic surgery, and retrovirus injections. Concentrated BAG stock, with titer 3.4×10^4 cfu/ml (assayed with NIH3T3 cells, without polybrene) were produced as previously described (Levison and Goldman, 1993). Sprague–Dawley rat pups (0–1 d postnatal; the day of birth being P0) were anesthetized by immersion in ice water for 7 min, positioned in a stereotactic apparatus modified for neonatal rats (Heller et al., 1979) and kept cold with ice packs. After deflecting the scalp, 1 microliter of retroviral stock was injected unilaterally or bilaterally into the forebrain SVZ with a 10 μl Hamilton syringe using stereotactic coordinates of 0.7 mm anterior and 1.9 mm lateral to bregma at a depth of 1.9 mm. All injections were performed at these coordinates, which places virus within the forebrain SVZ at the level of the septal nuclei. Scalp incisions were closed with Vetbond tissue adhesive and the pups revived by warming and returned to the mother.

Tissue fixation and histology. Animals were anesthetized with a mixture of xylazine (55 mg/kg) and ketamine (10 mg/kg) and sacrificed by intracardiac perfusion via an intracardiac route with RPMI culture medium containing 6 U/ml heparin followed by 3% paraformaldehyde in 0.1 M phosphate buffer, pH 7.35. The brains were removed, fixed overnight, and transferred to PBS. A block of tissue rostral to the optic chiasm was sectioned at 300 or 50 μm intervals on a vibratome (Technical Products International, series 1000). For X-gal histochemistry sections were rinsed in PBS containing 2 mM $MgCl_2$ and incubated overnight at 28°C in a solution containing 1 mg/ml 5-bromo-4-chloro-3-indolyl-beta-D-galactopyranoside (X-gal; Molecular Probes, Eugene, OR), 30 mM potassium ferrocyanide, 30 mM potassium ferricyanide, and 2 mM $MgCl_2$ in PBS. The sections were rinsed two times with PBS, once with PBS containing 3% DMSO, followed by two rinses with PBS prior to being mounted on glass slides with Aquamount (Lerner Laboratories). Unless specified reagent grade chemicals were purchased from Sigma Chemical Corporation, St. Louis, MO.

Immunohistochemistry. Animals were sacrificed by intracardiac perfusion using a fixative containing 3% paraformaldehyde and 0.5% glutaraldehyde in 0.1 M PIPES, 2 mM $MgCl_2$, pH 7.3. A mouse monoclonal anti-β-galactosidase (mouse IgG2A, used at 1:20 dilution; Promega, Madison, WI) antibody was used in conjunction with antibodies against vimentin (mouse monoclonal IgG1, clone V9, used at 1:20 dilution; Boehringer-Mannheim, Indianapolis, IN), nestin (Rat 401, mouse monoclonal IgG1 kindly provided from Susan Hockfield or from Developmental Studies Hybridoma Bank, Iowa City, IA; tissue culture supernate used undiluted), glial fibrillary acidic protein (mouse monoclonal IgG1, used at 1:50 dilution; Boehringer Mannheim, Indianapolis, IN), ED1 (mouse monoclonal IgG1, ascitic fluid used at 1:300 dilution; Harlan-Bioproducts, Indianapolis, IN) or a biotinylated griffonia simplicifolia isolectin B4 (Sigma). Fluorescein and rhodamine conjugated secondary antibodies were obtained from Southern Biotechnology Associates (Birmingham, AL). Fluorochrome-conjugated avidin was obtained from Vector Laboratories (Burlingame, CA). Staining was performed on 50 μm vibratome sections permeabilized in 0.2% Triton X-100 in PBS for 30 min and blocked for 1 hr in 10%BSA, 10% normal goat serum in PBS. Overnight incubations with primary and secondary antibodies was carried out at 4°C using PBS containing 10% lamb serum, 10% fetal bovine serum. Stained sections were viewed with an Olympus BH-2 microscope equipped with epifluorescence optics. In some cases, X-gal stained sections were further processed for immunocytochemistry for vimentin using an ABC peroxidase method, visualizing reaction product with diaminobenzidine.

Results

Early migration of cells from the SVZ into white matter and neocortex

As in previous experiments, a stereotactic injection of the retroviruses into the forebrain SVZ selectively labeled cells in that area (see Levison and Goldman, 1993). Since the infected cells were located in a discrete region of the germinal zone, migration from the SVZ could be inferred upon finding labeled cells in brain regions distant from the injection site. In this study we used a concentrated viral stock in order to label a large number of SVZ cells, reasoning that it would be easier to examine migrational paths and antigen expression of a large population. To study the early stages of SVZ cell migration, we examined coronal sections of the injected brains at 24 hr and 2.5, 3.5, and 7 d postinjection (dpi). With increasing times after injection, more cells appeared outside of the SVZ and more had migrated longer distances.

Brains examined 24 hr postinjection showed the great majority of X-gal positive cells concentrated in the SVZ, and only a few in adjacent parenchyma (Fig. 1). Occasional cells were observed in the cortex just dorsal to the SVZ and in white matter just dorsal or lateral to the SVZ (Fig. 1*A,B*).

By 2.5 dpi, although most of the labeled cells still remained in the SVZ, a larger proportion of the labeled cells were found in the overlying white matter, cortex dorsal to the SVZ, and lateral white matter (Fig. 2). A few cells had even reached the dorsal pial surface by this time, a distance of about 2 mm from the SVZ (not shown). In addition, cells were observed in lateral cortex. We presume for two reasons that these cells first migrated along lateral white matter and then turned to colonize the cortex. First, we saw very few cells in the dorso-lateral cortex at this stage, but would have expected to have seen many if cells had first migrated dorsally and then turned to migrate transversely through the cortex. Second, cells had migrated several mm along white matter by 2.5 dpi. Many of the cortical cells appeared to be arranged in radially oriented groupings.

By 3.5 dpi, a more widespread distribution was seen, with cells now appearing in the dorso-lateral neocortex and lateral white matter and a few in the corpus callosum between the hemispheres (Fig. 3). Labeled cells were distributed throughout all cortical layers. In some areas, groups of cells were arranged radially, with respect to the pial surface (Fig. 3). Cells were present in the lateral white matter and a small number of cells had migrated into the striatum adjacent to SVZ. By 7 dpi, labeled cells were distributed thoughout cortex and white matter (Fig. 4). Some cells still remained in the SVZ at this time.

Multiple sections through individual brains revealed that dorsal migration, from the SVZ into the overlying cortex, occurred in the more anterior sections, while migration into lateral cortex took place in both anterior and more posterior sections. The most posterior sections that contained labeled cells showed migration largely into white matter, with only a few cortical cells (Figs. 2, 4).

It is unlikely that the labeled cells that appeared in the cortex were labeled during the injection process from virus that was deposited along the needle track. First, labeled cortical cells were found in distant sections anterior and lateral to the location of the injection site. Second, if cells were labeled during injection, we would expect to see the largest concentration of these cells along the injection track, and this was never the case. Third, we have not seen cells at the pial surface or in the upper cortical

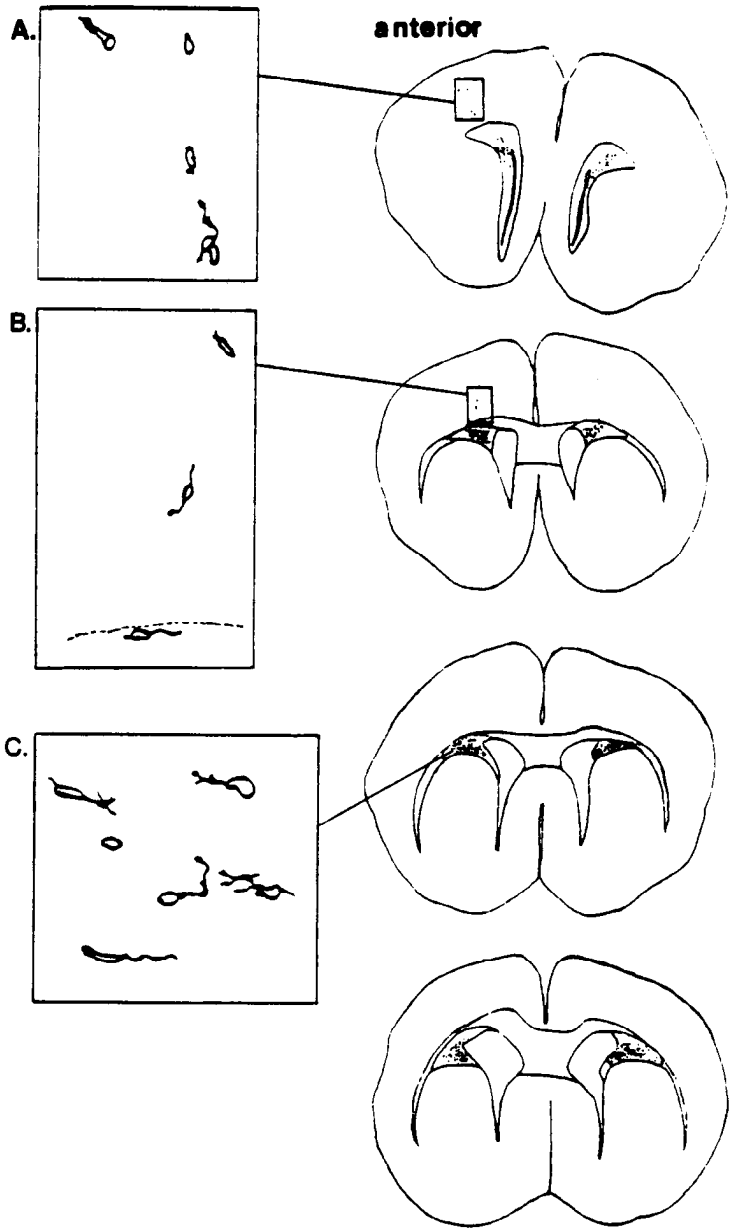

Figure 1. Location of retrovirus labeled progenitors 24h post infection. SVZ cells were labeled with the BAG virus at P0 and brains were processed for X-gal histochemistry 24 hr later. The distribution of labeled cells in consecutive 300 μm coronal sections of one brain (of a total of four) is depicted here in camera lucida drawings. Each dot represent one labeled cell. The most anterior section is at the top. The second section from the top contains the site of injection. *A*, Morphology of four cortical cells is indicated. *B*, Morphology of three cells in white and gray matter; the border between cortex and white matter is indicated by a *dotted line*. *C*, Morphology of representative SVZ cells.

layers 24 hr postinjection. Fourth, when the SVZ target was missed during the injection, we did not find X-gal positive cells in any location in the brain. In fact, deliberately injecting retrovirus into cortex did not result in labeling (Levison and Goldman, 1993).

Morphologies of early migrating cells

We examined the morphologies of those X-gal labeled cells that resided in the SVZ and those that appeared in the cortex and white matter within the first few days after injection. Most of the labeled SVZ cells appeared unipolar, some additionally displaying short side branches (Figs. 1*C*, 4*B*). Nuclei were round or oval or sometimes irregular and indented. Occasional apolar cells and mitotic cells were seen. At all times, within the 7 d period of analysis, we continued to observe labeled cells in the SVZ, indicating that the retroviral-labeled cells did not emigrate synchronously. The morphology of these SVZ cells appeared the same at all times. Thus, labeled cells that remained in the SVZ at 7 dpi displayed the same morphologies as those in the SVZ at earlier times.

In contrast, the population of labeled cells that had moved into the cortex and white matter appeared more heterogeneous, with increasing numbers of morphologically more complex cells at longer times postinjection (compare Figs. 1, 3, 4). Thus, after 24 hr, the cells that have emigrated from the SVZ into the dorsal cortex and lateral white matter still retain an immature morphology similar to that exhibited by labeled cells residing in the SVZ (Fig. 1). At 2.5 and 3.5 dpi, although many cells in cortex and white matter looked like the unipolar SVZ cells, often with the single process oriented toward the pial surface or along the white matter parallel to axonal pathways, others appeared more complex (Fig. 3). Some were bipolar, their processes also oriented radially in the cortex or along axonal tracks in white matter. Some cells, even at these early times, showed morphological features consistent with early astrocytic differentiation. We found cells in cortex with several processes emanating from the

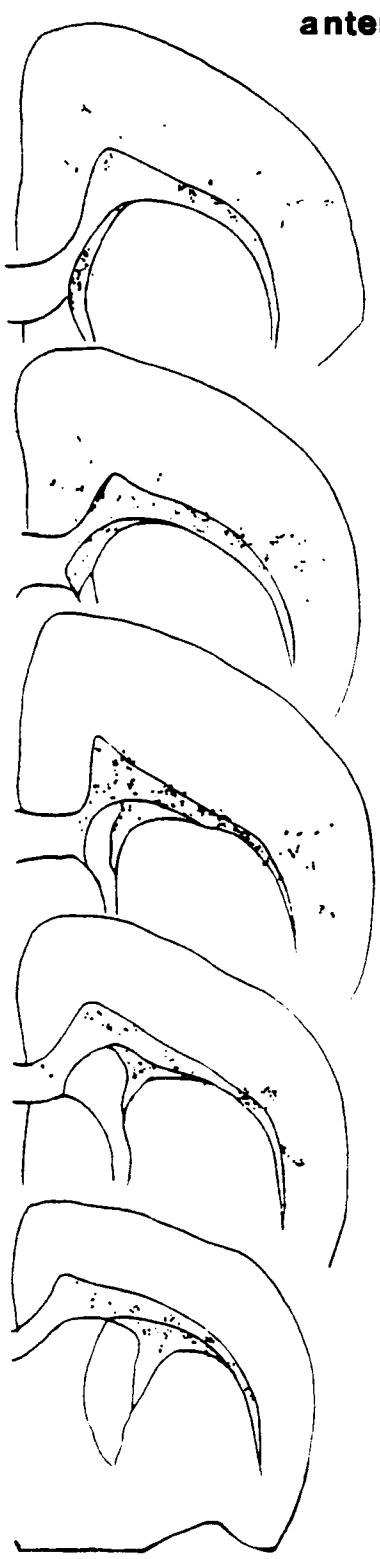

Figure 2. Location of labeled cells 2.5 d postinfection. SVZ cells were labeled with BAG at P0 and brains processed at 2.5 d later. Camera lucida drawings of 300 μm consecutive sections are shown from one brain (of a total of six). Each dot represents a single, labeled cell. The most anterior sections is at the top.

cell body; each process in turn displayed several small branches (Fig. 3*B,D*). A few cells showed processes in close proximity to blood vessels with small expansions along vessels, suggesting an astrocyte-like endfoot contact (Fig. 3*A*). At these early times after injection it is difficult to determine quantitatively the relative proportions of the various morphological forms in the cortex, since this proportion appeared to vary from animal to animal. Nevertheless, a general pattern was clear, in which a progression to more and more complex forms took place over the first week after injection.

Evidence for mitotic division of labeled cells in the cortex was seen. A number of cells showed closely apposed nuclei and rounded-up forms (Fig. 3*B,D*). We also observed sets of two similar cells with nuclei in contact, suggesting that these represented recently separated siblings. X-Gal labeled mitotic figures were occasionally seen in SVZ, white matter, and cortex (not shown).

By 7 dpi, larger numbers of more complex, branching forms had emerged in the cortex (Fig. 4). These bore the morphologies of astrocytes (as discussed in Levison and Goldman, 1993). However, less complex, unipolar and bipolar cells were still readily seen at this time. For example, a unipolar cell with the morphology of the progenitors in the SVZ was found in the cortex 5 dpi (Fig. 5*C*).

In the developing white matter 3.5 dpi, many X-gal labeled cells displayed an immature, unipolar morphology. However, others had larger, round nuclei and only a small amount of perinuclear cytoplasm (Fig. 3*C*). These cells bore fine processes, which could not be easily resolved with the X-gal stain. We did not observe cells with the complex, branched morphologies of those found in the cortex. Myelin sheaths were not detectable at 3.5 dpi. By 7 dpi, the white matter contained a more complex mixture of cells. A few oligodendrocytes connected to myelin sheaths had developed (Fig. 4*D*). Rows of "interfascicular" oligodendrocytes had also formed (Fig. 4*D*). Other cells, typically in small groups, displayed the round perikarya of immature oligodendrocytes and were surrounded by thin, blue processes (Fig. 4*D*). Some processes were clearly seen as connected to perikarya, others apparently not. We interpret these cells as early myelinating oligodendrocytes, with a few thin processes, not well resolved with the X-gal stain. Most of the early myelinating and myelinating oligodendrocytes appeared in the white matter lateral and medial to the SVZ. In contrast, immediately dorsal to the SVZ, in the large expanse of white matter referred to as the "cingulum," X-gal labeled cells showed a less mature morphology: large cell bodies, sparse perinuclear cytoplasm, round or often indented nuclei, and few processes (Fig. 4*C*).

In summary, cells retained an immature morphology as they migrated into white matter and cortex. In the cortex, the earliest morphologically identifiable cells appeared to be astrocytic, with multipolar shapes and blood vessel contacts. We know from previous work that some SVZ cells develop into cortical oligodendrocytes (Levison and Goldman, 1993). However, at these early times after injection, we were not able to identify morphologically mature oligodendrocytes in the cortex. At all times during the first week postinjection, labeled immature cells were present in cortex, and it is therefore likely that some of these would have differentiated into oligodendrocytes at later times. In contrast, many labeled cells in the white matter displayed features of immature oligodendrocytes, but not astrocytes, consistent with our previous findings that SVZ cells preferentially differ-

Figure 3. Location and morphologies of labeled cells 3.5 d postinfection. SVZ cells were labeled with BAG at P0–1 and brains processed 3.5d later. Three 300 μm thick sections, close to the injection site, from three separate brains are shown (*1–3*) (a total of five brains were examined). *A*, Morphologies of two cortical cells with astrocytic morphology, with processes apposed to blood vessels. *B*, A cluster of cells near the pial surface. *C*, Morphologies of a group of cells in subcortical white matter. *D*, Morphology of a radially oriented group of cells near the pial surface.

entiate into oligodendrocytes in white matter (Levison and Goldman, 1993; Levison et al., 1993).

Intermediate filament expression of retroviral labeled cells

Because many of the cells that migrated into the cortex soon after infection appear to develop into astrocytes, we characterized the infected cells further with antibodies to nestin, vimentin, and GFAP types of intermediate filament proteins. Experiments were performed with double-label indirect immunofluorescence with antibodies to β-galactosidase and to one of the filament proteins. We chose for this analysis to examine brains at 5 dpi when clusters of labeled cells at different stages of differentia-

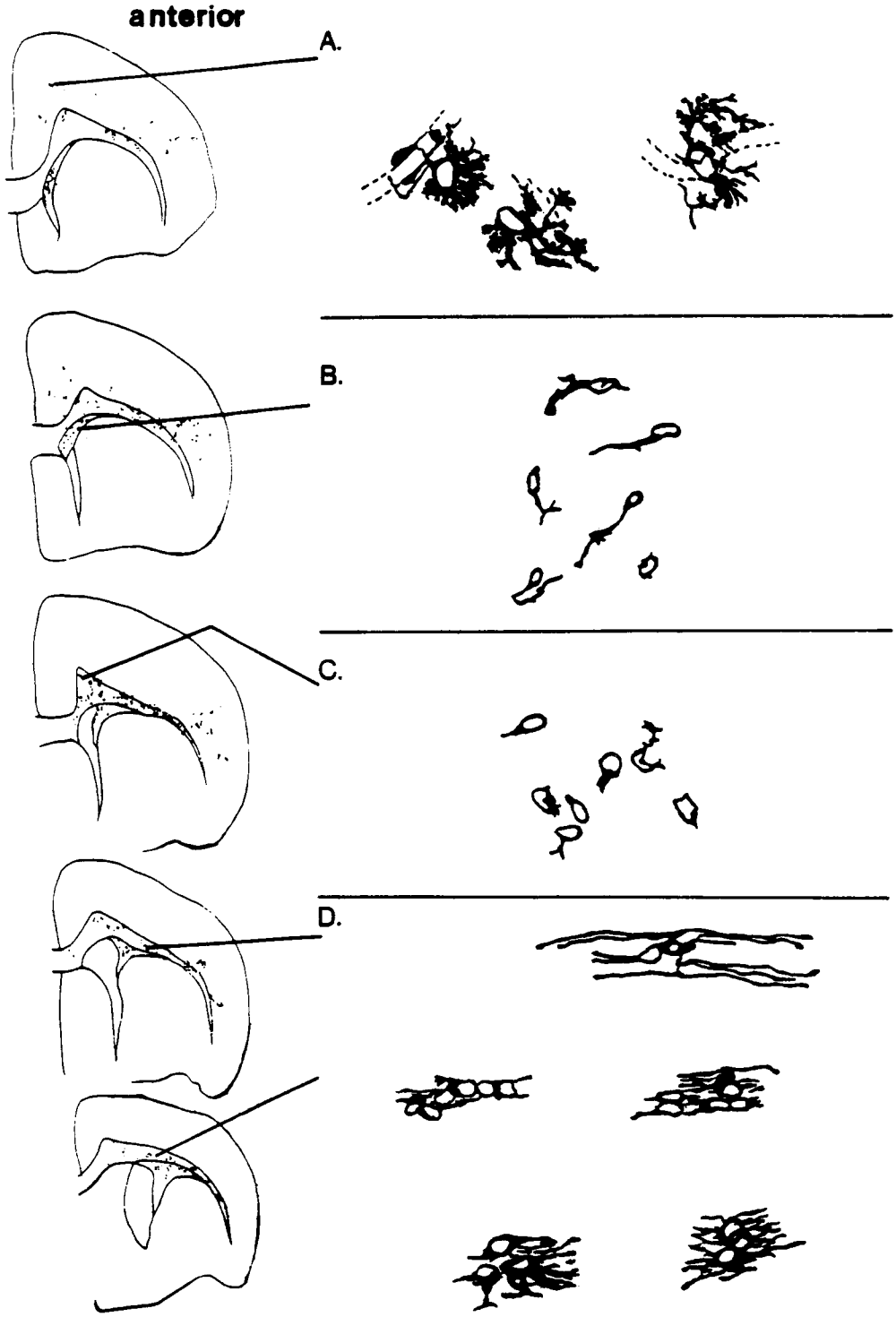

Figure 4. Location and morphologies of labeled cells 1 week postinfection. SVZ cells were labeled with BAG at P0–1 and processed 1 week later. Consecutive 300 μm sections from one brain (from a total of six) are shown, with each dot representing a labeled cell. *A*, Morphology of three cortical astrocytes, with processes contacting vessels. *B*, Appearance of a group of SVZ cells. *C*, Typical morphologies of labeled cells found in the cingulum. *D*, Cells with the morphologies of oligodendrocytes were found in the white matter at this time. Mature, myelinating oligodendrocytes, clusters of "interfascicular" oligodendrocytes, and early myelinating oligodendrocytes are all observed (see text for detailed descriptions). Fewer labeled cells were seen in this brain than in the brains depicted in Figure 3, presumably due to the variable nature of the numbers of SVZ cells initially infected.

tion were readily found. An example of such cortical clusters is shown in Figure 5. The initially infected population of unipolar cells in the SVZ did not bind any of the anti-filament antibodies (Fig. 6, Table 1). Although both nestin and vimentin immunoreactivity were present in the SVZ at these early postnatal times, the filaments were found in processes of cells that did not correspond to those of the retroviral labeled progenitors. Many of the nestin+ and vimentin+ processes in the SVZ were aligned in parallel, radial arrangements, indicating that they were expressed by radial glia, or subventricular astrocytes with processes in the SVZ. Retroviral infected cells in white matter did not bind any of the anti-intermediate filament antibodies (Fig. 6, Table 1). Some of these white matter cells assumed the same unipolar morphology as SVZ cells, as noted above, or bipolar forms, with processes aligned along the fiber tracts. The white matter cells with larger, round nuclei, which we interpret as immature oligodendrocytes, did not express any of the filaments.

In contrast to our observations in SVZ and white matter, we did find infected cells in the cortex that expressed nestin and vimentin (Fig. 6, Table 1). All of the cortical cells that displayed

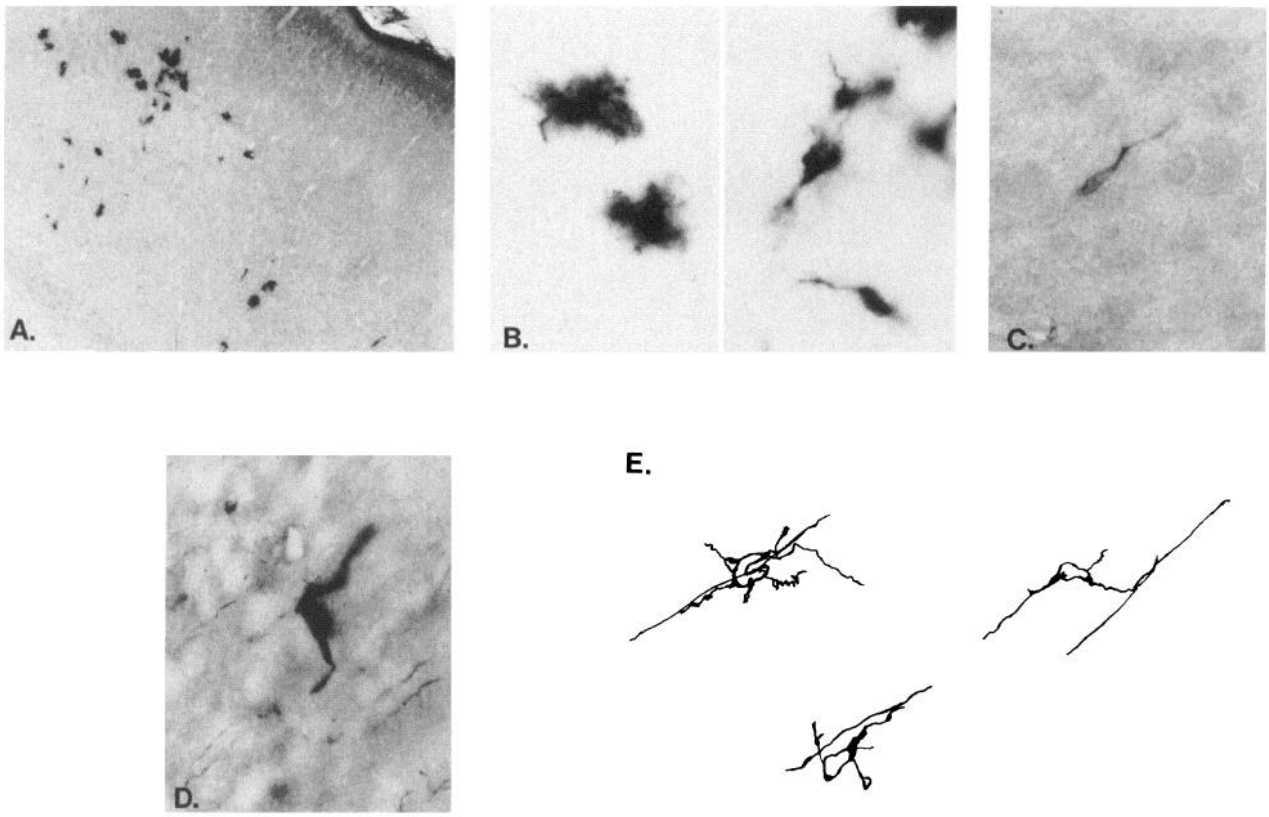

Figure 5. Labeled cells colonizing the cortex 5 d postinfection. SVZ cells were labeled with BAG at P0–1 and brains were processed 5 d postinfection. Sections were stained with X-gal and with the anti-vimentin antibody (using a peroxidase method). *A*, Low power view of the cortex in a section close to the injection site, showing several clusters of X-gal labeled cells, displaying a mixture of morphologies, 41×. *B*, Higher magnification of details of these cells shown in *A*. Immature-appearing, unipolar cells coexist with more mature astrocytes, 412×. *C*, A unipolar cell in the cortex. Its morphology is similar to cells found in the SVZ, 412×. *D*, An X-gal labeled bipolar cell in the cortex. The cell's processes are arranged so that each contacts a radial glial process; the cell body lies in between, 412×. *E*, Camera lucida drawings of three immature cells in the cortex and radial glial processes nearby. Some of their processes show close alignment or contact with radial glial processes.

multiprocess-bearing morphologies contained detectable vimentin immunoreactivity (38/38 cells analyzed). Most, but not all, were nestin+ (48/54 cells). The population of infected cells that appeared morphologically immature was more complex in its filament expression. While many of the cortical unipolar and bipolar cells did not express filament proteins, a few did (not shown). We observed no GFAP immunoreactivity in labeled cells, although perhaps this is to be expected, since GFAP is expressed later than the vimentin in rodent CNS development (Dahl et al., 1981; Schnitzer et al., 1981). GFAP immunoreactivity was readily detectable at this time, however (not shown). Presumably, if we had waited longer, some of the β-gal+ cells would have expressed GFAP (Levison and Goldman, 1993).

Immunostaining with the antibody against vimentin also allowed us to visualize the spatial relationships between labeled cells and radial glia. In a number of cases we found close apposition of unipolar or bipolar cells in the cortex to vimentin+ radial processes (Fig. 5). In one example, a single cell contacts two parallel radial glia, each of the cell's processes lying on a separate radial glia with the cell body resting in between (Figs. 5*D,E*).

Do the β-gal+ SVZ cells develop into microglia?

We considered the possibility that the retrovirus was labeling microglia either already present in the SVZ region (Boya et al., 1991; Ling and Wong, 1993) or derived from circulating blood monocytes that invaded the CNS as a result of injury of the injection. We analyzed the population of β-gal labeled cells for the coexpression of ED-1. ED-1 is detectable in the "ameboid" microglia in the early postnatal rat CNS (Flaris et al., 1993). We found that none of the β-gal+ cells in the SVZ, white matter, and cortex was positive for ED-1 (Table 1, Fig. 7). We easily observed a large number of ED-1+ cells in the brain parenchyma, especially in the white matter region above the SVZ and in the subpial area. Most of the ED-1+ cells displayed a round morphology, typical of ameboid microglia, while a few exhibited a more elongated shape. In the cortex, we also observed ED-1+ pericytes, which were also β-gal-negative (not shown). We detected the same population of (β-gal-negative) microglial cells using the isolectin *Griffonia simplicifolia* (B4), although this staining was lighter than the one obtained with the ED-1 antibody (not shown).

Discussion

Migration of glial progenitors from the SVZ

Recombinant retroviruses have allowed us to visualize patterns of migration, morphologies, and antigenic profiles of the cells that migrated from the forebrain SVZ. Our current observations support the idea that postnatal glial progenitors utilize radial glial tracks to migrate, just as neuronal progenitors had done previously. First, the simple, unipolar morphology of cells that first appear in white and gray matter is similar, if not identical, to

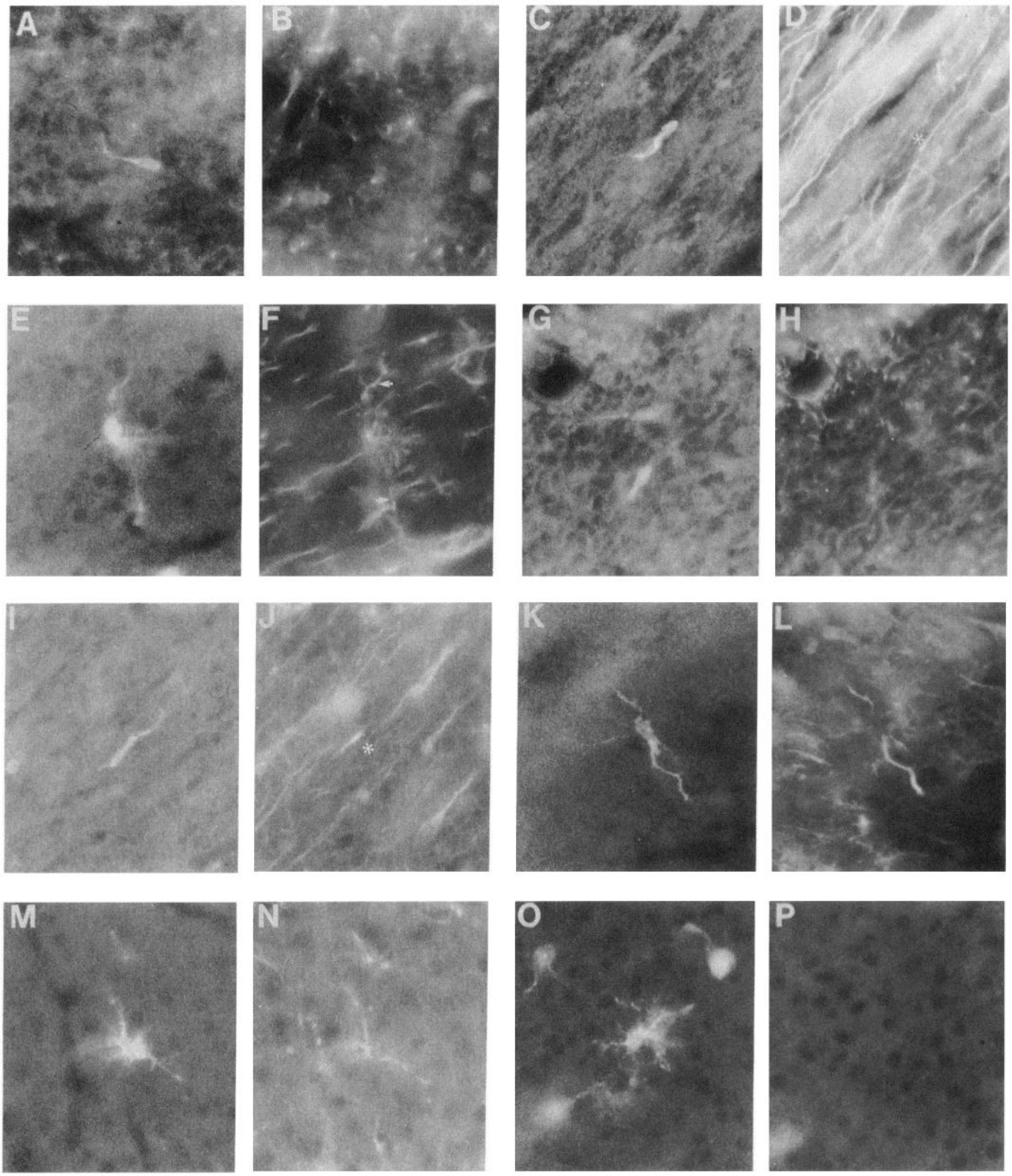

Figure 6. Intermediate filament expression by retrovirus labeled SVZ cells and their progeny at 5 dpi. SVZ cells were labeled with BAG at P0–1 and brains processed for immunofluorescence 5 dpi. Coexpression of β-gal and each of the IF proteins was monitered by double-label immunofluorescence. *A–F*, β-gal/vimentin double label. *A* and *B*, Progenitor βgal+ (*A*), but vimentin− (*B*), note the many vimentin+ processes, most viewed obliquely, in the SVZ. *C* and *D*, Unipolar cell in white matter β-gal+ (*C*), but vimentin− (*D*). *Asterisk* in *D* shows position of body of cell shown in *C*; again, note many vimentin+ processes belonging to radial glia. *E* and *F*, Multiprocess cell in cortex is β-gal+ (*E*), vimentin+ (*F*); *arrows* in *F* represent two processes of cell shown in *E*. *G–N*, β-gal/nestin double label. *G* and *H*, Two progenitors in the SVZ are β-gal+ (*G*), nestin− (*H*); note nestin+ processes, most cut in cross-section in this field. *I* and *J*, A bipolar cell in white matter is β-gal+ (*I*), but nestin− (*J*). *Asterisk* in *J* represents body of cell shown in *I*. *K–N*, Multiprocess cells in the cortex are β-gal+ (*K, M*), nestin+ (*L, N*). *O* and *P*, A cluster of multiprocess cells, one of which is in plane of focus, is β-gal+ (*O*), GFAP− (*P*). The white matter in this brain showed many GFAP+ astrocytes (not shown). All panels at 340×.

Table 1. Immunofluorescence analysis of retroviral labeled cells *in vivo*

	vim+/total βgal+	Nestin+/ total	GFAP+/ total	ED-1/ total
SVZ cells	0/46	0/65	0/25	0/35
White matter				
Unipolar/bipolar	0/12	0/10	0/8	0/10
Round	0/5	0/4	0/3	0/5
Cortex				
Unipolar/bipolar	6/15	4/16	0/4	0/7
Complex	38/38	48/54	0/42	0/30

SVZ cells were labeled with the BAG retrovirus at P0 and brains were processed for immunofluorescence at 5 dpi as described in Materials and Methods. Coexpression of the retroviral β-galactosidase and each of the other markers was monitored by double label immunofluorescence. The data were expressed as the number of double positive cells per total βgal+ cells examined. A total of five brains were examined for vimentin and nestin and two for GFAP and ED-1.

that of the migratory cells that leave the ventricular zone during prenatal development (Austin and Cepko, 1990; Misson et al., 1991a; Fishell et al., 1993; Walsh and Cepko, 1993). These cells in prenatal brain have been assumed to be postmitotic, migrating neuroblasts, but it is possible that some are glial progenitors or multipotential progenitors. Second, many of the unipolar and bipolar, X-gal–labeled cells are radially aligned in the cortex, and radially oriented groups were common. Third, labeled cells were often aligned along radial glial pathways (Misson et al. 1991a). SVZ cells migrated into the cortex just dorsal to the SVZ and into and along the lateral white matter before migrating into lateral cortex. This pattern of colonization of the cortex is similar to that proposed for neuronal migration, based upon thymidine labeling, in which cortical neuron progenitors migrate laterally along white matter before turning into the cortex to migrate radially (Bayer et al., 1991). Fourth, using time-lapse video microscopy we have observed postnatal SVZ cells migrating along radial processes in a cell culture system (S. Newman, M. Zerlin, and J. E. Goldman, unpublished observations).

At very early time postinfection we observed few or no labeled cells in the dorso-lateral cortex, but this region became populated later. It is possible that at these later times progenitors located in lateral white matter ascend into the cortex along radial fibers. If that is the case, why progenitors do not move along such a pathway immediately is unclear. However, tangential dispersion of progenitors already present in the cortex may also contribute to colonize the dorso-lateral region. In fact, previous studies on neuroblast migration *in vivo* (Walsh and Cepko, 1988; Gray and Sanes, 1991) and in living slices (O'Rourke et al., 1992) have postulated the importance of a tangential component to neuroblast migration. Our observations of labeled glial progenitors with processes contacting two parallel radial glial processes suggests that glial progenitors may be able to disperse tangentially by using adjacent radial processes to anchor themselves.

A few labeled cells had reached positions close to the pial surface by 2.5 dpi. Assuming these represent cells that integrated

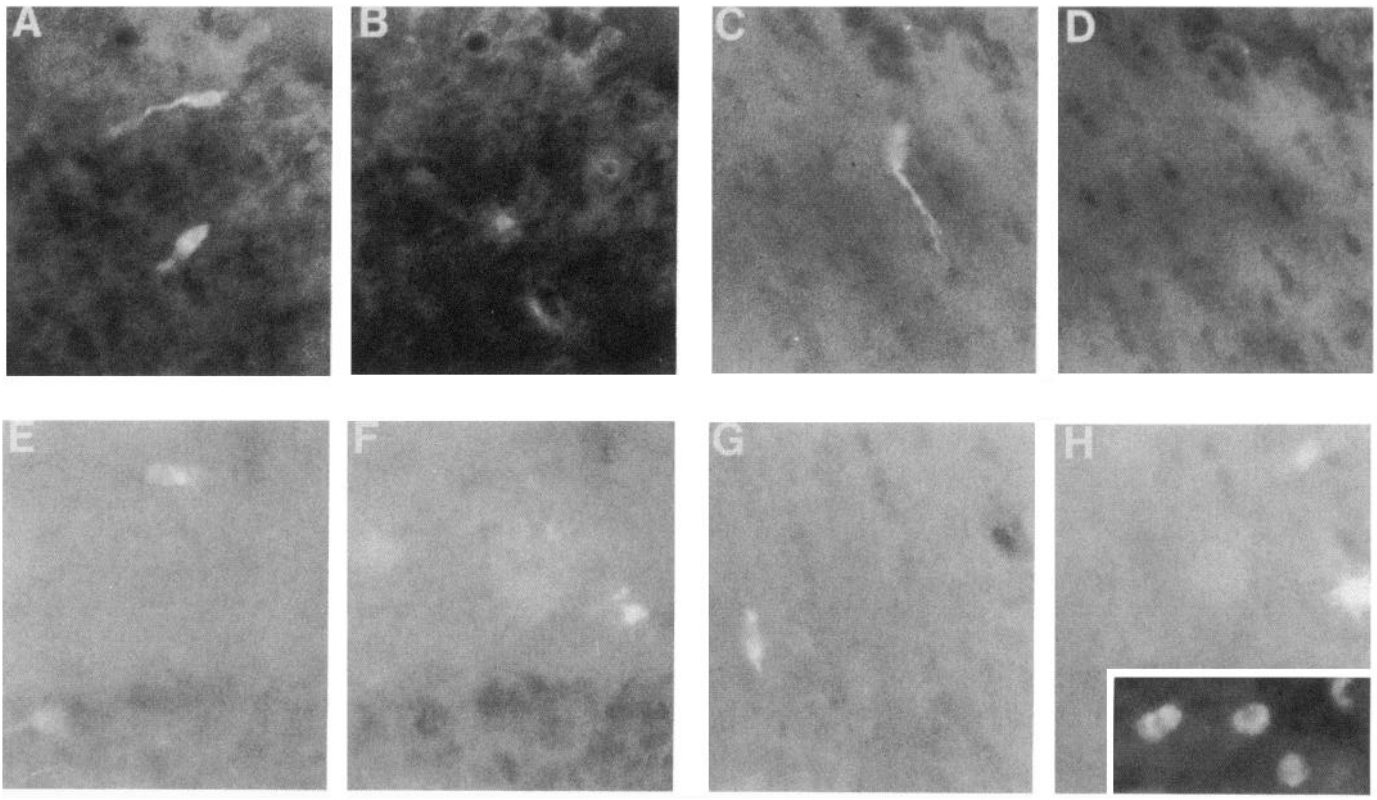

Figure 7. Retroviral labeled SVZ cells and their progeny do not express the microglial marker ED-1. SVZ cells were labeled with BAG at P0–1 and brains processed 5 dpi. Coexpression of β-gal and ED-1 was assessed by double immunofluorescence. *A* and *B*, Two progenitors in the SVZ express β-gal (*A*), but not ED-1 (*B*). *C* and *D*, A unipolar cell in white matter is β-gal+ (*C*), ED-1− (*D*). *E–H*, Two round-oval cells in white matter are β-gal+ (*E, G*), but ED-1− (*F, H*). *F* and *H* also show round, ED-1+ cells. The *inset* in *H* shows ED-1+ cells in white matter in these brains. All panels at 340×.

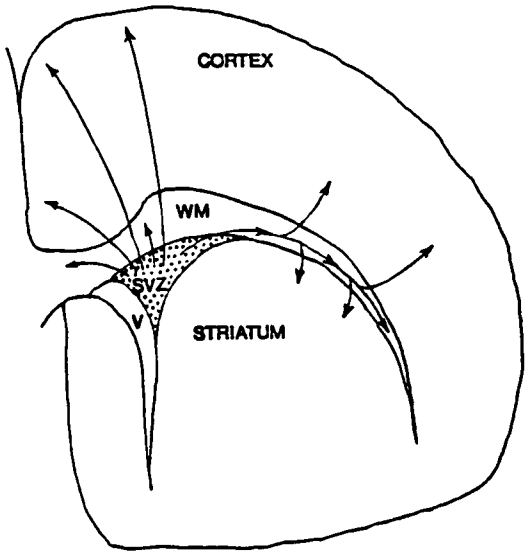

Figure 8. Diagram of migrational patterns of postnatal SVZ cells. This simplified diagram depicts migrational patterns of postnatal SVZ cells into neighboring white matter (*WM*), cortex, and striatum. Most of the migration takes place in a coronal plane (see Levison et al., 1993). The pattern is similar to that described for the migration of cells from germinal zones in the prenatal CNS (Bayer et al., 1991; Misson et al., 1991a), with prominent radial and lateral components. Tangential migration is also possible, but is not noted on this figure.

the virus within hours after injection and emigrated from the SVZ also within hours, and given that the pial surface is about 2 mm from the SVZ injection site, these cells would have had to have traveled at a minimum rate of about 1 mm/d. This rate compares closely with the average rate of granule cell migration along radial glia *in vitro* of 0.8 mm/d (Edmonson and Hatten, 1987) and of O-2A progenitors from optic nerve in culture on poly-L-lysine of 0.5 mm/d, with (transient) maximal rates up to 2.4 mm/d (Small et al., 1987). Migration rates along white matter tracts appear to be similar, since distances that labeled SVZ cells had moved into lateral white matter were about the same as distances moved into cortex. Figure 8 depicts in a simplified summary form the pathways we believe postnatal SVZ cells take as they colonize adjacent white matter, cortex, and striatum. We have emphasized the radial and lateral components, but do not exclude tangential migration as well.

Morphogenesis and blood vessel interactions during migration

Labeled cells that appeared in the cortex displayed a wide range of morphologies. At early times after injection, many of the cells appeared unipolar, similar to the forms of SVZ cells. Because these cells were observed over the first few days after injection, we infer that these represent the earliest migrating forms. Although most labeled cells that had appeared in the cortex 2.5–3.5 dpi were simple in form, a few displayed a complex, multiprocess morphology, indicating that morphological differentiation to a multiprocess state can be accomplished within 2 d. Some of these also appeared to contact blood vessels, suggesting an early stage of astrocyte differentiation. The cells that contacted blood vessels at this early age did not show the highly complex, multibranched morphology seen in astrocytes of older animals, however, suggesting that blood vessel attachment precedes the full elaboration of a complex cell shape. Whether blood vessel contact occurs at an early stage in astrocyte development from multipotential progenitors and even whether blood vessel contact plays a role in progenitor differentiation into astrocytes needs to be explored in more detail.

By 7 dpi astrocytic cells with multiprocess, branched morphologies had emerged. These were interspersed with cells of a simpler morphology. Two phenomena could account for this heterogeneity. Since there is continuous emigration of labeled cells out of the SVZ during the first week, one would expect to see a mixture of cells in different stages of development, particularly if glia do not populate the neocortex in a systematic, laminar fashion. Alternatively, the rate at which cells differentiate may vary, so that some remain immature in cortex while (related) cells differentiate into astrocytes or oligodendrocytes. The continued presence of immature cells is consistent with much previous data on the presence of dividing cells in the adult mammalian neocortex (Kaplan and Hinds, 1980). Furthermore, oligodendrocyte clusters in cortex appear to increase severalfold in size from 1 month to 9 months, indicating continued generation of glia from progenitors (Levison and Goldman, unpublished observations).

The transformation of radial glia has been thought to account for the generation of large numbers of astrocytes in cortex and white matter in early postnatal life (Voigt, 1989; Misson et al., 1991b). At no time did we see labeled radial glial forms, nor did we in previous studies. Thus we conclude that astrocytes can also be generated directly from the SVZ without a proximate radial glial intermediate form (Levison and Goldman, 1993; Luskin and McDermott, 1994). During the first few days after retroviral injection, the cortex contained radially oriented, bipolar and multipolar labeled cells. These resemble what have been described in Golgi and immunocytochemical studies of developing cortex as "transitional" forms between radial glia and the astrocytic derivatives of radial glia (Choi and Lapham, 1978; Schmechel and Rakic, 1979; Misson et al., 1988, 1991b). Yet the X-gal labeled cells we observed originated in the SVZ and did not arrive in the cortex through a radial glial intermediate. Thus, it is possible that some of the "radial glial" and early "astrocytic" cells previously noted are really SVZ cells that had migrated out into cortex and had begun to differentiate into astrocytes. It is unlikely that radial glia are not infected by retroviruses or that they suppress the reporter gene since Halliday and Cepko (1992) did visualize radial glia in striatum with prenatal injections of retrovirus, and Gray and Sanes (1992) consistently labeled radial glia in the chick optic tectum. It is likely, however, that existing radial glia are not mitotically active during the perinatal period when we injected the retrovirus.

Many previous studies have used light and electron microscopy and immunostains to characterize glial precursors, and by studying the distribution of transitional forms have inferred migrational patterns (see for example: Vaughn, 1969; Paterson et al., 1973; Skoff et al., 1976; LeVine and Goldman, 1988a,b; Reynolds and Wilkin, 1988; Skoff, 1990; Hardy and Reynolds, 1991; Fulton et al., 1992). The simple, X-gal–labeled cells we observed in the SVZ, developing white matter and cortex look like the immature neuroectodermal cells described in electron micrographs (Vaughn, 1969; Privat and Leblond, 1972; Skoff et al., 1976; Sturrock and Smart, 1980; LeVine and Goldman, 1988a,b). These cells resemble the process-bearing GD3-ganglioside-labeled cells present in immature white matter (LeVine and Goldman, 1988a,b; Reynolds and Wilkin, 1988; Hardy and Reynolds, 1991). A population of large, round, irregular cells in white matter also reacts with anti-GD3 antibodies (LeVine and

Goldman, 1988a; Reynolds and Wilkin, 1988; Hardy and Reynolds, 1991). As noted (Wolswijk, 1994), some of these cells are likely to represent macrophages. The round, β-gal+ cells in developing white matter were ED-1 negative. They displayed a high nuclear:cytoplasmic ratio and lacked the granular cytoplasm, characteristic of macrophages, and are morphologically distinct from ameboid microglial cells. We interpret these cells to be glial progenitors (Fig. 7), most likely immature oligodendrocytes. These results, together with the fact that we only observe X-gal+ oligodendrocytes and astrocytes in brain analyzed four weeks postinjection (Levison and Goldman, 1993; Zerlin, unpublished observations) support the contention that we are not labeling microglia or macrophages, but rather neuroectodermal progenitors.

Intermediate filament expression

We did not find vimentin expression in the labeled SVZ cells or in the unipolar or bipolar cells in white matter, but only in cortical cells that exhibited a complex, multiprocess shape and in a fraction of the simpler (unipolar or bipolar) cortical cells. Some of these simple cells were clearly contacting the pial surface or the wall of a blood vessel. This expression pattern is consistent with previous studies of SVZ cells *in situ* (LeVine and Goldman, 1988a) and of astrocyte development, which show vimentin expression prior to GFAP expression (Dahl et al., 1981; Schnitzer et al., 1981; Bovolenta et al., 1984). The fact that immature CNS cells express vimentin *in vitro* (Raff et al., 1983; Hardy and Reynolds, 1991) may represent a response to culture conditions, since vimentin gene expression is induced by exposure to serum, platelet-derived growth factor and phorbol esters through a *cis*-regulatory element (Franke et al., 1979, Rittling et al., 1989; van de Klundert et al., 1992). Vimentin RNA and protein levels are reduced significantly in epithelial kidney cells forced to grow in suspension (Ben-Ze'ev, 1984), suggesting that vimentin gene expression is controlled by signals generated by attachment of cells to a substrate (or by the concerted effects of growth factors and substrates).

We were also unable to detect nestin expression by retroviral-labeled progenitors either in the SVZ or in subcortical white matter. We did observe strong nestin immunoreactivity in these regions, however, but it did not correspond to the β-gal labeled cells, but rather mostly to radial glial processes, as originally described (Hockfield and McKay, 1985). Several reports have used nestin as a marker to identify neuroectodermal progenitors. However, in most cases, neural tissues containing these progenitors have been established in culture in the presence of serum or purified growth factors (Cattaneo and McKay, 1990; Reynolds et al., 1992; Stemple and Anderson, 1992). These *in vitro* conditions may induce the expression of nestin by progenitors, as has been reported for O-2A progenitors cultured in the presence of PDGF and basic FGF or B104 conditioned medium (Gallo and Armstrong, 1995). Nestin+ cells have been identified in embryonic neural tube preparations fixed immediately after tissue dissociation (Frederiksen and McKay, 1988). By this approach, the subpopulations of neuroectodermal progenitors cannot easily be distinguished from other cell types (radial glia, for example), which coexist with progenitors in the germinal zone. A recent report by Gallo and Armstrong (1995) used tissue prints of neonatal rat brain to identify cells that were A2B5+ and nestin+. In contrast, the β-gal–labeled unipolar and bipolar cells that we found in white matter did not contain nestin. This apparent discrepancy might be explained in several ways. (1) The β-gal–labeled cells in white matter may express lower levels of nestin than is detectable under our experimental conditions (although we did observe strong nestin immunoreactivity in radial glia and cortical, process-bearing cells). (2) A small proportion of white matter glial progenitors express nestin, but we failed to analyze enough cells to find them. (3) It is possible that the tissue printed nestin+ bipolar cells were actually in the cortex and not in white matter. We did find a small proportion of bipolar cortical cells containing nestin. (4) The A2B5+ cells reported by Gallo and Armstrong (1995) may represent a different subset of progenitors than the ones we are detecting by retroviral gene transfer.

Although we were unable to detect nestin expression in labeled progenitors in SVZ or immature cells in white matter, we did observe that the majority of the process-bearing cells in the neocortex did express this intermediate filament type. As in the case of vimentin, nestin expression seems to be an early event in the differentiation of glial progenitors along an astrocyte pathway. Perhaps an increase in filaments is necessary for stabilization of major astrocyte processes during the early phases of astrocyte differentiation.

References

Altman J (1966) Proliferation and migration of undifferentiated precursor cells in the rat during postnatal gliogenesis. Exp Neurol 16: 263–278.

Angevine JB Jr, Sidman RL (1961) Autoradiographic study of cell migration during histogenesis of cerebral cortex in the mouse. Nature 192:766–768.

Austin CP, Cepko CL (1990) Cellular migratrion patterns in the developing mouse cerebral cortex. Development 110:713–732.

Bayer SA, Altman J, Russo RJ, Dai X, Simmons JA (1991) Cell migration in the rat embryonic neocortex. J Comp Neurol 307:499–516.

Ben-Ze'ev A (1984) Differential control of cytokeratins and vimentin synthesis by cell–cell contact and cell spreading in cultured epithelial cells. J Cell Biol 99:1424–14233.

Berry M, Rogers AW (1965) The migration of neuroblasts in the developing cerebral cortex. J Anat 99:691–709.

Bovolenta P, Liem RKH, Mason CA (1984) Development of cerebellar astroglia: transitions in form and cytoskeletal content. Dev Biol 102: 248–259.

Boya J, Calvo JL, Carbonell AL, Borregon A (1991) A lectin histochemistry study on the development of rat microglial cells. J Anat 175:229–236.

Cattaneo E, McKay R (1990) Proliferation and differentiation of neuronal stem cells regulated by nerve growth factor. Nature 347:762–765.

Choi BH, Lapham LW (1978) Radial glia in the human fetal cerebrum: a combined Golgi, immunofluorescent, and electron microscopic study. Brain Res 148:295–311.

Curtis R, Cohen J, Fok-Seang J, Hanley MR, Gregson NA, Reynolds R, Wilkin GP (1988) Development of macroglial cells in rat cerebellum. I. Use of antibodies to follow early *in vivo* development and migration of oligodendrocytes. J Neurocytol 17:43–54.

Dahl D, Rueger DC, Bignami A (1981) Vimentin, the 57,000 molecular weight protein of fibroblast filaments, is the major cytoskeletal component of immature glia. Eur J Cell Biol 24:191–196.

Edmondson JC, Hatten ME (1987) Glial-guided granule neuron migration *in vitro*: a high-resolution time-lapse video microscopic study. J Neurosci 7:1928–1934.

Edwards MA, Yamamoto M, Caviness VS Jr (1990) Organization of radial glia and related cells in the developing murine CNS. Neuroscience 36:121–144.

Fishell G, Mason CA, Hatten ME (1993) Dispersion of neural progenitors within the germinal zones of the forebrain. Nature 362:636–638.

Flaris NA, Densmore TL, Molleston MC, Hickey WF (1993) Characterization of microglia and macrophages in the central nervous system of rats: definition of the differential expression of molecules using standard and novel monoclonal antibodies in normal CNS and in four models of parenchymal reaction. Glia 7:34–40.

Franke WW, Schmid E, Winter S, Osborn M, Weber K (1979) Widespread occurrence of intermediate-sized filaments of the vimentin type in cultured cells from diverse vertebrates. Exp Cell Res 123:25–46.

Frederiksen K, McKay RDG (1988) Proliferation and differentiation of rat neuroepithelial precursor cells *in vivo*. J Neurosci 8:1144–1151.

Fulton BP, Burne JF, Raff MC (1992) Visualization of O-2A progenitor cells in developing and adult rat optic nerve by quisqualate-stimulated cobalt uptake. J Neurosci 12:4816–4833.

Gallo V, Armstrong RC (1995) Developmental and growth factor-induced regulation of nestin in oligodendrocyte lineage cells. J Neurosci 15:394–406.

Gray GE, Sanes JR (1991) Migratory paths and phenotypic choices of clonally related cells in the avian optic tectum. Neuron 6:211–225.

Gray GE, Sanes JR (1992) Lineage of radial glia in the chicken optic tectum. Development 114:271–283.

Gressens P, Richelme C, Kadhim HJ, Gadisseuz J-F, Evrard P (1992) The germinative zone produces the most cortical astrocytes after neuronal migration in the developing mammalian brain. Biol Neonate 61:4–24.

Halliday AL, Cepko CL (1992) Generation and migration of cells in the developing striatum. Neuron 9:15–26.

Hardy R, Reynolds R (1991) Proliferation and differentiation potential of rat forebrain oligodendrocyte progenitors both *in vitro* and *in vivo*. Development 111:1061–1080.

Hatten ME (1990) Riding the glial monorail: a common mechanism for glial-guided neuronal migration in different regions of the developing mammalian brain. Trends Neurosci 13:179–184.

Heller A, Hutchens JO, Kirby ML, Karapas F, Fernandez C (1979) Stereotactic electrode placement in the neonatal rat. J Neurosci Methods 1:41–76.

Hicks SP, D'Amato CJ (1968) Cell migrations to the isocortex in the rat. Anat Rec 160:619–633.

Hockfield S, McKay RDG (1985) Identification of major cell classes in the developing mammalian nervous system. J Neurosci 5:3310–3328.

Imamoto K, Paterson JA, Leblond CP (1978) Radioautographic investigation of gliogenesis in the corpus callosum of young rats. I. Sequential changes in oligodendrocytes. J Comp Neurol 180:115–138.

Kaplan MS, Hinds JW (1980) Gliogenesis of astrocytes and oligodendrocytes in the neocortical grey and white matter of the adult rat: electron microscopic analysis of light radioautographs. J Comp Neurol 193:711–727.

LeVine SM, Goldman JE (1988a) Embryonic divergence of oligodendrocyte and astrocyte lineages in developing rat cerebrum. J Neurosci 8:3992–4006.

LeVine SM, Goldman JE (1988b) Spatial and temporal patterns of oligodendrocyte differentiation in rat cerebrum and cerebellum. J Comp Neurol 277:441–455.

Levison SW, Goldman JE (1993) Both oligodendrocytes and astrocytes develop from progenitors in the subventricular zone of postnatal rat forebrain. Neuron 10:201–212.

Levison SW, Chuang C, Abramson B, Goldman JE (1993) The migrational patterns and developmental fates of glial precursors in the rat subventricular zone are temporally regulated. Development 119:611–622.

Ling EA, Wong WC (1993) The origin and nature of ramified and amoeboid microglia: a historical review and current concepts. Glia 7:9–18.

Luskin MB, McDermott K (1994) Divergent lineages for oligodendrocytes and astrocytes originating in the neonatal forebrain subventricular zone. Glia 11:211–226.

Misson J-P, Edwards MA, Yamamoto M, Caviness VS Jr (1988) Identification of radial glial cells within the developing murine central nervous system: studies based upon a new immunohistochemical marker. Dev Brain Res 44:95–108.

Misson J-P, Austin CP, Takahashi T, Cepko CL, Caviness VS Jr (1991a) The alignment of migrating neural cells in relation to the murine neopallial radial glial fiber system. Cereb Cortex 1:221–229.

Misson J-P, Takahashi T, Caviness VS Jr (1991b) Ontogeny of radial and other astroglial cells in murine cerebral cortex. Glia 4:138–148.

O'Rourke NA, Dailey ME, Smith SJ, McConnell SK (1992) Diverse migratory pathways in the developing cerebral cortex. Science 258: 299–302.

Paterson JA, Privat A, Ling EA, Leblond CP (1973) Investigation of glial cells in semithin sections. III. Transformation of subependymal cells into glial cells, as shown by radioautography after H3-thymidine injection into the lateral ventricle of the brain of young rats. J Comp Neurol 149:83–102.

Privat A, Leblond CP (1972) The subependymal layer and neighboring region in the brain of the young rat. J Comp Neurol 146:277–302.

Raff MC, Miller RH, Noble M (1983) A glial progenitor cell that develops *in vitro* into an astrocyte or an oligodendrocyte depending on culture medium. Nature 303:390–396.

Rakic P (1972) Mode of cell migration to the superficial layers of the fetal monkey neocortex. J Comp Neurol 145:61–83.

Reynolds R, Wilkin GP (1988) Development of macroglial cells in rat cerebellum. II. An *in situ* immunohistochemical study of oligodendroglial lineage from precursor to mature myelinating cell. Development 102:409–425.

Reynolds BA, Tetzlaff W, Weiss S (1992) A multipotent EGF-responsive striatal embryonic progenitor cell produces neurons and astrocytes. J Neurosci 12:4565–4574.

Rittling SR, Coutinho L, Amram T, Kolbe M (1989) AP-1/jun binding sites mediate serum inducibility of the human vimentin promoter. Nucleic Acids Res 17:1619–1633.

Schmechel DE, Rakic P (1979) A Golgi study of radial glial cells in developing monkey telencephalon: morphogenesis and transformation into astrocytes. Anat Embryol 156:115–152.

Schnitzer J, Franke WW, Schachner M (1981) Immunocytochemical demonstration of vimentin in astrocytes and ependymal cells of developing and adult mouse nervous system. J Cell Biol 90:435–447.

Skoff RP (1990) Gliogenesis in rat optic nerve: astrocytes are generated in a single wave before oligodendrocytes. Dev Biol 139:149–168.

Skoff RP, Price DL, Stocks A (1976) Electron microscopic autoradiographic studies of gliogenesis in rat optic nerve. II. Time of origin. J Comp Neurol 169:313–334.

Small RK, Riddle P, Noble M (1987) Evidence for migration of oligodendrocyte-type-2 astrocyte progenitor cells into the developing rat optic nerve. Nature 328:155–157.

Stemple DL, Anderson DJ (1992) Isolation of a stem cell for neurons and glia from the mammalian neural crest. Cell 71:973–985.

Sturrock RR, Smart IHM (1980) A morphological study of the mouse subependymal layer from embryonic life to old age. J Anat 130:391–415.

van de Klundert FAJM, vanEldik GJ, Pieper FR, Jansen HJ, Bloemendal H (1992) Identification of two silencers flanking an AP-1 enhancer in the vimentin promoter. Gene 122:337–343.

Vaughn JE (1969) An electron microscopic analysis of gliogenesis in rat optic nerve. Z Zellforsch 94:293–324.

Voigt T (1989) Development of glial cells in the cerebral wall of ferrets: direct tracing of their transformation from radial glia into astrocytes. J Comp Neurol 289:74–88.

Walsh C, Cepko CL (1988) Clonally related cortical cells show several migration patterns. Science 241:1342–1345.

Walsh C, Cepko CL (1992) Widespread dispersion of neuronal clones across functional regions of the cerebral cortex. Science 255:434–440.

Walsh C, Cepko CL (1993) Clonal dispersion in proliferative layers of developing cerebral cortex. Nature 362:632–635.

Wolswijk, G (1994) GD3+ cells in the adult rat optic nerve are ramified microglia rather than O-2A adult progenitor cells. Glia 10:244–249.